Design and modelling of photobioreactor for the treatment of carpet and textile effluent using *Diplosphaera mucosa VSPA*

Virendra Singh[1] · Pradeep Srivastava[1] · Abha Mishra[1]

Abstract

The current study investigated the potential of one less explored microalgae species, *Diplosphaera mucosa VSPA*, for treating carpet and textile effluent in a conventionally designed 10 L bubble column photobioreactor. To the best of our knowledge, this is the first study to evaluate COD (chemical oxygen demand) removal efficiency by microalgae in carpet effluent. To evaluate *D. mucosa VSPA's* potential, its growth and bioremediation efficacy were compared to those of a well-known strain, *Chlorella pyrenoidosa*. *D. mucosa* VSPA outperformed *C. pyrenoidosa* in both effluents, with the highest biomass concentration reaching 4.26 and 3.98 g/L in carpet and textile effluent, respectively. *D. mucosa VSPA* also remediated 94.0% of ammonium nitrogen, 71.6% of phosphate phosphorus, and 91.9% of chemical oxygen demand in carpet effluent, approximately 10% greater than that of *C. pyrenoidosa*. Both species also removed more than 65% of colour from both effluents, meeting the standard set by governing bodies. Microalgae growth and substrate removal patterns in the photobioreactor were simulated using photobiotreatment and the Gompertz model. Simulation results revealed that photobiotreatment was the better-fit model, concluded based on the coefficient of regression value and the second-order Akaike information criterion test. Modelling studies can assist in increasing the performance and scale-up of the photobioreactor.

Abbreviations

Abs.	Absorbance
BOD	Biological oxygen demand
COD	Chemical oxygen demand
Dia	Diameter
HRT	Hydraulic retention time
NH_4^+–N	Ammonium nitrogen
NRE	Nitrogen removal efficiency
PBRs	Photobioreactors
PO_4^{3-}–P	Phosphate phosphorus
PRE	Phosphorus removal efficiency
RE	Removal efficiency
STP	Sewage Treatment Plant (STP)
TE1	Textile effluent containing acid yellow dye
TE2	Textile effluent containing acid orange dye
TE3	Textile effluent containing basic pink dye
HRAP	High-rate algal pond

✉ Abha Mishra
abham.bce@itbhu.ac.in

Pradeep Srivastava
pksrivastava.bce@iitbhu.ac.in

1   School of Biochemical Engineering, IIT(BHU), Varanasi, India

Introduction

Rapid industrialization and globalisation have caused a rise in energy demand and a significant increase in wastewater production. According to the United Nations Report "Valuing Water", 4000 km³/year of wastewater is generated worldwide (Schmidt 2019). A significant portion of wastewater is generated by industries, which include the tannery industry (Pena et al. 2020), the textile industry (Yadav et al. 2019), the brewery industry (Song et al. 2020), the carpet industry (Chinnasamy et al. 2010), dairy wastewater (Brar et al. 2019a), and many more. Over 70–80% of the wastewater is improperly treated before being discharged directly into freshwater streams (Schmidt 2019). Discharge of a large amount of nutrients leads to eutrophication, which deteriorates both flora and fauna's health in aquatic bodies. Some of these pollutants include dyes from textile effluent that are carcinogenic (Pathak et al. 2015; Jose and Archanaa 2019). Various conventional methods, including physicochemical

and biological, are available for wastewater treatment, but very few of them are cost-effective techniques (Mazhar et al. 2019). Many of them require high energy, generating chemically contaminated waste (Wan et al. 2016; Mohsenpour et al. 2021). An alternate strategy, microalgae-based wastewater treatment, has recently gained widespread attention (Singh and Mishra 2020). Microalgae not only remediate pollutants from wastewater but also assist in resource recovery by generating valuable biomass (Singh et al. 2019). Numerous studies have shown that microalgae can be used to treat a variety of industrial effluents (El-Kassas and Mohamed 2014; Mohammadi et al. 2019; Krishnamoorthy et al. 2019; Hemalatha et al. 2019; Leng et al. 2020; Song et al. 2020; Han et al. 2021). However, several microalgal species are still unexplored, as their number varies from 200,000 to 500,000 (Venkatesan et al. 2015). Exploring more microalgal species will lead to the discovery of more robust strains that will treat wastewater more efficiently. Determining the best-suited species for the remediation of industrial effluents is crucial.

Large-scale microalgae-based wastewater treatment is usually carried out using raceway ponds or photobioreactors (PBR). Raceway ponds are simple in design, durable, and cost-efficient (Behera et al. 2019). One of the types of raceway ponds, high-rate algal pond (HRAP), is being implemented for microalgae-based wastewater due to its better efficiency than other ponds (Santiago et al. 2013). A study predicted that biofuel production from microalgae biomass cultivated in raceway ponds would be energetically favourable when wastewater is used as a nutrient source (Sturm and Lamer 2011). Open raceway ponds, however, are more susceptible to contamination and evaporative loss (Patil et al. 2021). Compared to raceway ponds, photobioreactors are less prone to contamination and more efficient than raceway ponds (Xu et al. 2009). Even microalgae biomass productivity is 2–5 times higher in PBR (Jones and Harrison 2014). Various types of PBR are available for microalgae cultivation, including tubular reactors, plastic bags, and column and rectangular airlifts (Mehmood et al. 2014; Huang et al. 2017). Among these PBRs, bubble column photobioreactors are widely used as they are easy to design, construct, and operate compared to other PBRs (Fu et al. 2012). They provide efficient heat and mass transfer characteristics while occupying less floor area (López-Rosales et al. 2017). But there might be a problem of light diffusion during dense culture, which can be fixed by internal illumination and by improving the mixing process (Tuantet et al. 2019). Therefore, in addition to exploring new species, the discussion of photobioreactors' design and modelling parameters will play a crucial role in the scale-up of the microalgae-based wastewater treatment process.

The current study assessed the potential of one of these understudied species, taking into account the points mentioned, *Diplosphaera mucosa*, belonging to the class *Trebiouxyphyceae*, for treating carpet and textile effluent. A web of knowledge database search reported no publication related to the carpet and textile effluent treatment by *Diplosphaera mucosa*. The treatment process was carried out in a 10-L bubble column photobioreactor with a discussion of its design parameters. The design parameters discussed in the present study were the volumetric mass transfer coefficient, hydrodynamic properties, and light uptake rate. Biomass production and treatment efficiency of the *Diplosphaera mucosa* were compared to those of a well-known strain of the same class, *Chlorella pyrenoidosa*. The comparison will indicate whether the application of *Diplosphaera mucosa* for wastewater treatment will be feasible or not. The pattern of growth and substrate removal in the photobioreactor was described using the photobiotreatment model (PhBT) and Gompertz model (GP). The impact of wastewater's N/P ratio on biomass generation has also been explored and can be used as a critical design factor for reactor operation.

Methodology

Isolation and characterisation of strains

Diplosphaera mucosa strain was isolated from the inlet Sewage Treatment Plant (STP) in Bhagwanpur, Varanasi, India (25°16′21″ N, 83°0′16.92″ E). The sample was serially diluted and spread on agar plates containing Bold Basal Media (BBM) (Bischoff 1963). Plates were kept in an incubator at 25 °C and illuminated at 2500 lx intensity using LED tubes. Single colonies were picked up by examination under the microscope and streaked on fresh plates. The streaking process continued until a pure culture (free from contamination, confirmed under the microscope) was obtained. The sequence of the isolated culture was identified by 18 s rRNA sequencing and analysed by the BLAST programme. Analysis revealed that the strain showed close similarity with *Diplosphaera mucosa* (89.60%) and was therefore named *Diplosphaera mucosa* VSPA. The sequencing process was assisted by the National Collection of Industrial Microorganisms (NCIM), National Chemical Laboratory (NCL), Pune, India. A *Chlorella pyrenoidosa* strain was also procured from the NCIM. Its revival and cultivation steps have been explained in the supplementary section (S2.1).

Collection and characterisation of industrial effluents

Textile wastewater was collected from local textile industries in Varanasi, India (25°18′0″ N, 82°55′48″ E). Three variants of textile wastewater were collected: (a) textile effluent containing acid yellow dye (TE1); (b) textile effluent containing

acid orange dye (TE2); (c) textile effluent containing basic pink dye (TE3). Carpet industry effluent was collected from the Carpet Industry in Bhadohi, India (25°22′48″ N, 82°35′24″ E). The temperature of the wastewater samples was measured at the site of collection. The wastewater samples were filtered and put into storage for further use at 4 °C. Utilising standardised and globally accepted techniques, various wastewater sample parameters, including nitrogen, phosphorus, COD, and BOD, were determined (Rice et al.

2012). Important sample parameters involved in the study are presented in Table 1, and the rest are given in Table S1.

Photobioreactor construction

A cylindrical bubble column PBR was constructed using an acrylic tube purchased from a local hardware shop (Fig. 1). The total height of the reactor was 60 cm, with outer and inner diameters of 16 and 15 cm, respectively. The total

Table 1 Characterisation of different effluents through standard procedures

| S. no.	Parameter	Textile industry effluents			Carpet industry effluents	Legally admissible limit (Organization 2022)
		TE1	TE2	TE3		
1	Colour (visual)	Yellow	Orange	Dark pink	Reddish brown	Colourless
2	pH	8.1 ± 0.16	8.2 ± 0.16	8.2 ± 0.24	8.1 ± 0.08	6.5–8.5
3	Temperature (°C)	35 ± 1.63	35 ± 0.81	38 ± 0.81	35 ± 1.24	NA
4	Turbidity (NTU)	13.2 ± 0.16	14.3 ± 0.24	15.6 ± 0.32	210 ± 7.34	< 1
5	Nitrogen (ammonia) (mg/L)	45.2 ± 2.44	54.6 ± 3.26	46.2 ± 3.26	82.8 ± 1.63	0.2
6	Nitrogen (nitrate) (mg/L)	2.8 ± 0.16	2.12 ± 0.03	2.5 ± 0.24	3.5 ± 0.24	50
7	Phosphate (mg/L)	5.4 ± 0.32	6.3 ± 0.16	7.8 ± 0.73	9.3 ± 2.44	0.1
8	N/P ratio	8.3 ± 0.24	8.6 ± 0.32	5.92 ± 0.57	9.0 ± 0.32	NA
9	Dissolved oxygen (mg/L)	3.8 ± 0.32	1.6 ± 0.24	2.8 ± 0.32	1.6 ± 0.16	6.5–8
10	BOD_5 (mg/L)	78.8 ± 4.89	87.2 ± 3.26	83.6 ± 3.75	104 ± 6.53	1–2
11	COD (mg/L)	396 ± 16.32	372 ± 16.32	438 ± 14.69	1570 ± 16.32	10
12	Colour (Hazen)	142 ± 3.26	180 ± 9.79	202 ± 9.79	96 ± 4.08	NA
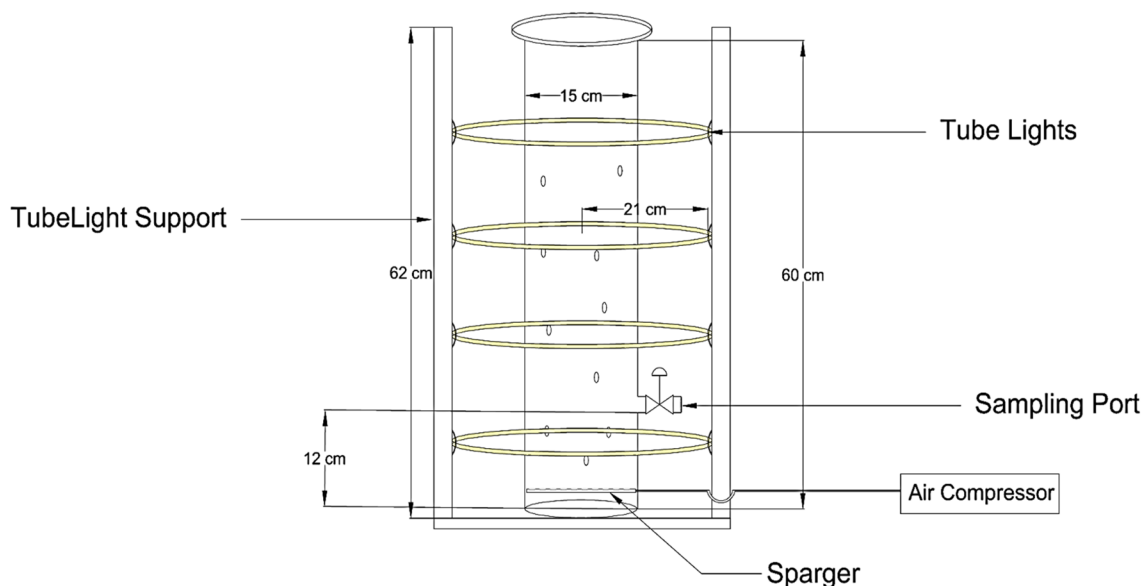
Fig. 1 Simplified diagram of the conventionally designed bubble column photobioreactor used in the present study (total height: 60 cm; inner diameter: 16 cm; outer diameter: 15 cm). Circular tube lights (30 W each) were used for illumination, and aeration was done using an air compressor through a sparger. Sampling port was used for daily sample analysis. (Designed in AUTOCAD 2023 Student Version)

volume of PBR was 10.6 L, with a working volume of 9 L. PBR was illuminated by four 30 W circular LED tube lights having a radius of 21 cm and providing 5000 lx intensity. The use of circular LED lights provides uniform light intensity around the reactor. A sampling port was provided at a height of 12 cm from the bottom. Aeration was done by an air compressor, and the sparger was placed at the bottom of the PBR. The bubble column PBR design parameters have been represented in Table 2 and were calculated as explained in the upcoming sections and supplementary section S2.2.

Light intensity and penetration loss

The total luminous flux (φ_v) passing through the reactor was calculated using Eq. (1):

$$\varphi_v = P \times \eta, \tag{1}$$

where, P stands for power in watts (W), and η indicates lumens per watt (lm/W).

Light uptake rate

The light uptake rate (q) was calculated using Eq. (2):

$$q = \frac{\varphi \cdot I_o \cdot A_o}{X}, \tag{2}$$

where, I_o is the total incident irradiance $\mu E/m^2$-s, φ is the proportion of photosynthetically available light (%), X is the biomass concentration (g/L), and A_o is the total area of irradiance (m^2).

Volumetric mass transfer coefficient ($K_L a$)

$K_L a$ is one of the most critical parameters for designing a photobioreactor. Under the same hydrodynamic conditions, the mass transfer coefficient (K_L) and the square root of the diffusivity (D) follow the penetration theory (Khoo et al. 2016). Microalgal density mainly depends on the mass transfer rate of O_2 and CO_2 across the gas–liquid interface. $K_L a$ (CO_2) is calculated using Eq. (3) (Baquerisse et al. 1999):

$$K_L a(CO_2) = \sqrt{\frac{D_{O_2}}{D_{CO_2}}} \times K_L a(O_2), \tag{3}$$

where, D_{O_2} and D_{CO_2} are 2×10^{-9} m^2/s and 2.41×10^{-9} m^2/s, respectively, at 298.15 K. $K_L a$ (O_2) can be calculated with the help of the dynamic gassing out technique method as shown by Eq. (4) (Sánchez Mirón et al. 2000):

$$K_L a(O_2) \cdot (t - t_o) = \ln \frac{(C^* - C_o)}{(C^* - C)}, \tag{4}$$

where, t and t_o are given and initial times, respectively, C_o indicates the initial dissolved concentration of O_2, C^* indicates the saturated dissolved concentration of O_2, and C indicates the dissolved concentration of O_2 at the given time t.

Hydrodynamic property

Various hydrodynamic properties such as interfacial area, gas hold up, bubble rise velocity, and bubble diameter also hold importance during PBR design. More details about these parameters have been explained in the supplementary section (S2.1).

Experimental procedure

Batch experiments were performed in conventionally designed PBR to determine both strains' pollutant removal efficiency (ammonium nitrogen, phosphate phosphorus, COD, and colour) and biomass productivity. For inoculum preparation, strains were cultivated in 900 ml of BBM (10% of the reactor working volume) and monitored till the culture reached the mid-log phase by measuring optical density at 680 nm. After that, the growing strains were used for inoculating the reactor filled with effluent. pH was monitored daily by measuring the pH of the samples withdrawn from the reactor and maintained at 7 using 1N HCl and 1N NaOH. Light intensity was maintained at 5000 lx intensity via an electric regulator, and the 12 h:12 h light/dark cycle was maintained manually. Light intensity was measured using a lux metre. The temperature of the chamber in which the reactor was kept was maintained at 25 °C

Table 2 Different design parameters were derived for the design of a conventional photobioreactor

S. no.	Design parameter	Design value
1	Height/diameter	4.064
2	Cross sectional area	0.017 m^2
3	Volume of reactor	0.0108 m^3
4	Light intensity	36.45 $\mu mol/m^2/s$
5	Light uptake	1.28 $\mu mol/s/(g/L)$
6	Airflow rate	0.2 vvm
7	Gas hold up ($\mathcal{E}$)	$\mathcal{E} = 0.0115$
8	Bubble diameter	$d_b = 0.0028$ m
9	Reynolds no. (Re)	933
10	Superficial gas velocity	$U_G = 0.078$ m/s
11	Bubble rise velocity	$U_b = 0.8$ m/s
12	Interfacial area (a)	$a = 29.9$ m^2

by an air conditioner and measured by dipping a mercury thermometer in the reactor. Air in the reactor was sparged at 3 L/min through an air compressor. The reactor operated until the stationary phase was achieved, which took around 10 days. The stationary phase was determined by measuring the optical density of the samples withdrawn daily from the reactor. Samples were randomly withdrawn from the reactor for microscopic analysis to determine the presence of contamination by other microbes. The reactor without inoculum was also operated for 10 days, which served as control. All experiments were performed in triplicate, and average values and standard deviations were used for further calculation.

Analytical techniques

Every day, a predetermined volume of culture was taken out of the sample port to track the production of biomass and the elimination of nutrients. By measuring the sample's absorbance (Abs) at 680 nm, the biomass concentration (Conc.) was calculated, as per Eq. (5.1) for *D. mucosa* and Eq. (5.2) for *C. pyrenoidosa*, respectively:

$$\text{Abs.} = 0.1324 \times \text{Conc.}, \tag{5.1}$$

$$\text{Abs.} = 0.1765 \times \text{Conc.} \tag{5.2}$$

These equations were derived experimentally by plotting a standard curve between absorption and the known concentration of biomass. Using the above biomass concentration value, biomass productivity and specific growth were calculated by Eqs. (6) and (7), respectively (Singh and Mishra 2020):

$$P = \frac{X_f - X_i}{t_f - t_o}, \tag{6}$$

$$\mu = \frac{\ln X_t - \ln X_o}{t_{f - t_o}}, \tag{7}$$

where X_t (g/L) represents the biomass concentration at time t (day), X_o (g/L) represents the initial biomass concentration, t_f and t_o represent the final and initial sampling times, respectively, and μ (/day) represents the specific growth rate. In the 6th equation, P represents productivity (g/L/day), and X_i and X_f are the initial and final conc. of biomass (g/L), respectively, at times t_i and t_f. In addition to biomass concentration, chlorophyll (Chl) content was also determined, as sometimes debris or solids present in the reactor may hinder in accurate biomass determination, as explained in supplementary Sect. 2.4.

Next, samples were centrifuged at 8000 rpm for 10 min to determine the nutrient level. After that, the pellet was discarded, and measurements were done using the supernatant. NH_4^+–N and PO_4^{3-}–P concentrations were measured by the standard spectrophotometric method described by phenate and vanadomolybdophosphoric acid, respectively (Rice et al. 2012). COD was measured by the close reflux titrimetric method (Rice et al. 2012). After determining the nutrient values, the removal efficiency (RE) of the nutrients was determined by Eq. (8), respectively:

$$\text{RE} = \frac{N_o - N_f}{N_o} \times 100, \tag{8}$$

where RE indicates the percent removal efficiency, and N_f and N_o indicate the final and initial nutrient concentrations (mg/L).

Mathematical modelling study

For determining the growth and substrate removal patterns from the reactor and validating the experimental results, kinetic modelling studies are necessary. In the present work, two non-linear mathematical models, the photobiotreatment model (PhBT) and the Gompertz model, were used for the kinetic study. Models also assist in the reactor design and scale of the process. The PhBT model is the modified Verhult logistic model that assumes nutrient removal by microalgae depends on the biomass productivity of microalgae. In contrast, the Gompertz model assumes that nutrient removal does not depend on biomass productivity. Biomass concentration and substrate removal determined by the PhBT model are expressed by Eqs. (9.1) and (9.2):

$$X = \frac{X_O X_m e^{pt}}{X_m - X_o + X_o e^{pt}}, \tag{9.1}$$

$$S = \frac{\left(\frac{X_o}{Y} + S_o\right)(S_o - S_{na}) - S_{na}(S_o - \left(\frac{X_o}{Y} + S_o\right))e^{pt}}{(S_o - S_{na}) - (S_o - \left(\frac{X_o}{Y} + S_o\right))e^{pt}}, \tag{9.2}$$

where, X (g/L) indicates the biomass concentration at time t, (days), X_o indicates the initial biomass concentration (g/L), X_m indicates the maximum biomass concentration (g/L), S (mg/L) indicates the substrate concentration at time t, S_o indicates the initial substrate concentration (mg/L), S_{na} indicates the non-assimilable substrate concentration (mg/L), Y indicates the biomass yield (g/mg), and p indicates the maximum specific growth rate (/day). The Gompertz model for biomass and substrate is expressed by Eqs. (10.1) and (10.2), respectively:

$$X = A \times \exp\left[-\exp\left\{\left(\frac{\mu_m \times \exp(1)}{A}\right) \times (\lambda - t) + 1\right\}\right], \tag{10.1}$$

$$S(t) = S_i + (S_f - S_o) \times \exp\left[-\exp\{k \times (\lambda - t) + 1\}\right], \tag{10.2}$$

where μ_m denotes the maximum specific growth rate (/day), λ is the lag time (day), A is the maximum biomass concentration (g/L), $S(t)$ is the substrate or nutrient concentration (mg/L) at time t (days), and k is the nutrient uptake rate or substrate utilisation rate (/day).

Statistical analyses

Experimental findings and error bars were plotted using Origin Lab (Version 2017). The significance of the differences between the examined cultures was assessed using the Student's paired t test. T test was carried out using Orgin Lab (Version 2017) at a significance level of 0.05. The models were solved using a non-linear regression method using the solver supplement of Microsoft Excel. Kinetic parameters were determined by minimising the sum of square errors. The coefficient of regression (R^2) is not enough to evaluate the fair comparison of the models, as the values of R^2 are nearly similar. Therefore, another criterion, the second-order Akaike information criterion (AICC) test, was used for model comparison as expressed by Eq. (11). The model with a lower AICC value is suggested to be a better one:

$$\text{AICC} = N\ln\left(\frac{\text{RSS}}{N}\right) + 2K + \frac{2K(K+1)}{N - K - 1}. \tag{11}$$

The sample size is denoted by N, the residual sum of squares is denoted by RSS, and the number of estimated parameters in the model is denoted by K.

Result and discussion

Biomass production

Algal biomass is thought to be a potentially useful resource for the production of biofuels. Identifying and improving factors that enhance the growth rate and higher lipid content makes microalgae an attractive tool for biofuel production. The nutrients in the wastewater are utilised by the microalgal species and assimilated for biomass production

and product formation (Singh et al. 2019). Figure 2 and Table 3 represent a comparative evaluation of the biomass production for *D. mucosa* VSPA and *C. pyrenoidosa* in different wastewater effluents. In all cases, *D. mucosa* VSPA has higher biomass productivity (1.2–1.5 folds) than *C. pyrenoidosa* ($p < 0.05$). *Diplosphaera* species were first isolated by P.A. Broady from Antarctic terrestrial habitats in 1983 (Raabová et al. 2016). Therefore, due to the source of their isolation, *Diplosphaera* species may easily adapt to the unfavourable environment of wastewater, leading to high biomass productivity. As per Fig. 2, nearly two days of lag phase were obtained in all effluents, possibly due to toxic elements in wastewater (mostly Azo dyes) (Singh et al. 2019). Therefore, microalgal species need some time to acclimate themselves to wastewater environments. Microbes adapt to the unfavourable environment of wastewater during the lag phase through various physiochemical changes, such as the creation of enzymes needed to assimilate substrates present in the medium (Japar et al. 2021). The stationary phase in all textile effluents for both species was obtained earlier than carpet effluent due to a lower nutrient concentration in textile effluents, as shown in Table 1, around the 8th day. In carpet effluent, the stationary phase was observed after the 9th day.

The highest biomass concentration was obtained in the case of carpet effluent, which was 4.26 g/L in *D. mucosa* VSPA culture and 4.02 g/L in *C. pyrenoidosa* culture. Among the three variants of textile wastewater, the highest biomass concentration of 3.98 g/L was obtained in TE1 by *D. mucosa* VSPA. In contrast, the lowest biomass concentration of 2.20 g/L was obtained in TE3 by *C. pyrenoidosa*. The reason for such a trend in biomass production is the high N/P ratio of carpet effluent. Based on Redfield's work, the typical stoichiometric formula of the microalgal biomass is $C_{106}H_{181}O_{45}N_{16}P$. As a result, the N/P ratio of the culture medium should be around 16:1 to obtain high biomass productivity (Klausmeier et al. 2004). The highest N/P ratio of 9.01:1 was detected in carpet effluent. Another reason can be the presence of azo dyes in textiles that inhibit microalgae growth. Among the three variants of textile effluent, the highest N/P ratio was detected in TE1, which was 8.37:1. The Same was reflected in the biomass production trend. Biomass productivity decreased or became nil when all effluents' N/P ratios reached below 5. In a 1.4 L laboratory-designed PBR, Wagner et al. (2021) evaluated the effects of various N/P ratios on the growth of *Chlorella sp.* during continuous cultivation. According to their findings, microalgae growth decreased when the N/P ratio was below 5.2:1
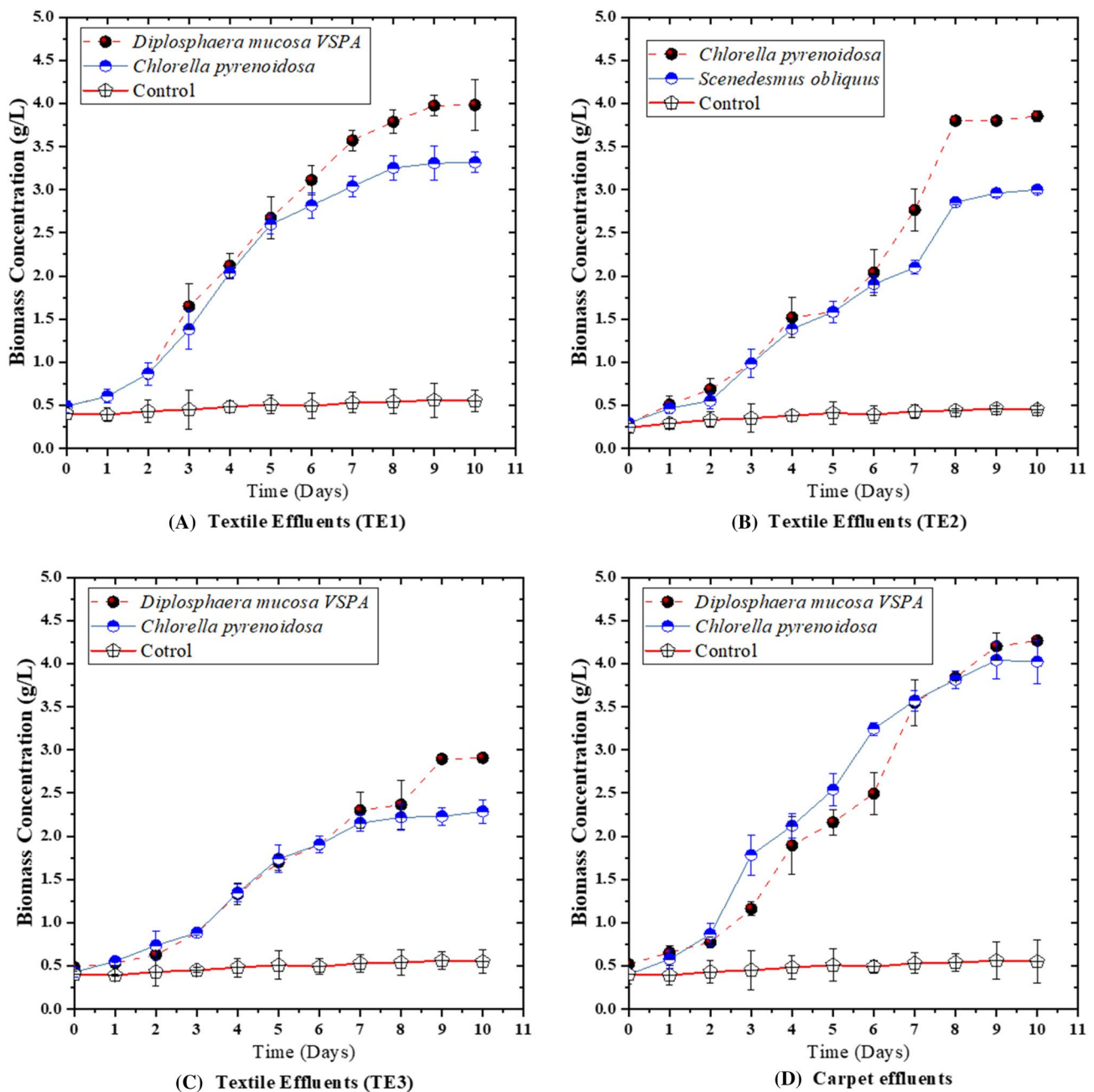
Fig. 2 The pattern of biomass concentration obtained during the cultivation of *D. mucosa* VSPA (red dashed line) and *C. pyrenoidosa* (blue dashed line) in: **A** textile effluent 1; **B** textile effluent 2; **c** textile effluent 3; **D** carpet effluent; The red solid line represents the control. Approximately two days into the log phase, and the stationary phase was achieved after the 8th day

(Wágner et al. 2021). In another study, Mayers et al. (2014) cultivated *Nannochloropsis* sp. at various N/P ratios ranging from 16:1 to 80:1. 16:1 and 32:1 N/P ratios supported a high microalgae growth rate, but a decrease in growth rate was detected at 64:1 and 80:1 N/P ratios (Mayers et al. 2014).

Pollutant removal

Wastewater contains ample nutrients that support microalgae growth and metabolism (You et al. 2022). A general diagram depicting the mechanism of nutrient removal by microalgae has been shown in Figure S1 (S1 indicates Supplementary

Table 3 Biomass and chlorophyll concentrations obtained during the cultivation of *D. mucosa* VSPA and *C. pyrenoidosa* in different effluents

Wastewater source	N/P ratio	*D. mucosa* VSPA			*C. pyrenoidosa*		
		Biomass concentration (g/L)	Chl *a* (µg/ml)	Chl *b* (µg/ml)	Biomass concentration (g/L)	Chl *a* (µg/ml)	Chl *b* (µg/ml)
TE1	8.37	3.98	2.98	0.89	3.31	2.68	1.08
TE2	8.6	3.85	2.76	1.06	3.00	2.86	1.09
TE3	5.92	2.90	2.82	1.12	2.28	2.72	1.08
Carpet effluents	9.01	4.26	3.72	1.34	4.02	3.52	1.24

file S1). Microalgal cells directly uptake ammonium nitrogen via the ammonium transporter. After that, glutamate and ATP facilitate the incorporation of NH_4^+–N into glutamine, which results in the formation of other amino acids and the generation of microalgae biomass (Sanz-Luque et al. 2015). Phosphorus is commonly present in wastewater as orthophosphate (PO_4^{3-}), which microalgae uptake via an active transport mechanism. This PO_4^{3-} gets incorporated into various organic compounds, such as ATP, through phosphorylation (Martínez Sancho et al. 1997).

Ammonium nitrogen (NH_4^+–N) removal

Microalgal cells require less energy to uptake NH_4^+–N than nitrate and nitrite. Therefore, NH_4^+–N becomes the preferential source of nitrogen for microalgae. NH_4^+–N present in effluents is transported into the cell by an ammonium transporter. Microalgal species utilise NH_4^+–N and finally convert it to ʟ-glutamate, which further converts into biomass (Singh et al. 2019). Hence, biomass productivity can be directly correlated with ammonium nitrogen removal. Table 4 represents the comparative evaluation of *D. mucosa* VSPA and *C. pyrenoidosa* for the assimilation of NH_4^+–N from different wastewater sources, and the pattern of removal is shown in Figure S2. It is evident from Table 4 that *D. mucosa VSPA* outperformed *C. pyrenoidosa* in all wastewater sources ($p < 0.05$). Due to the two-day lag phase, there was a slight decrease in ammonium removal due to the dependency of nutrient removal on microalgae growth. But after the second day, the NH_4^+–N concentration rapidly decreased

until day 10. The highest ammonium removal efficiency was obtained by *D. mucosa* VSPA in carpet effluent (94%) during the 10-day cultivation period, while it was 87.97% for *C. pyrenoidosa* in the same effluent. Carpet industrial units in Bhadohi, India (popularly known as the Carpet Capital of India), alone generate 7% of the total wastewater generated in the city (Vidyarthi et al. 2020). Therefore, *D. mucosa* species will be beneficial for carpet effluent treatment. Chinnasamy et al. (2010) cultivated 15 native algal isolates in a medium containing carpet industry effluent. The treatment method was highly effective, and more than > 96% of pollutants were remediated (Chinnasamy et al. 2010).

Among the three variants of textile effluent, the highest NH_4^+–N removal efficiency of $90.4 \pm 0.2\%$ was obtained in TE1 by *D. mucosa* VSPA during a 10 days cultivation period. A slightly lower RE of $90.2 \pm 0.1\%$ was obtained in TE2, and the lowest RE of $82.7 \pm 1.0\%$ was obtained in TE3. In the case of *C. pyrenoidosa*, the highest RE of $84.1 \pm 1.0\%$ was obtained in the case of TE2, with subsequent RE of $83.8 \pm 0.2\%$ in TE1 and $77.63 \pm 0.3\%$ in TE3. RE in the TE3 for both species was lower than other wastewater sources, possibly due to the low N/P ratio or more toxic compounds. Brar et al. (2019) cultivated three microalgal species, *Chlorella pyrenoidosa, Scenedesmus abundans, and Anabaena ambigua,* in 75% diluted textile effluent. Species were cultivated for 25 days, and 74.43% RE for nitrogen was obtained by *C. pyrenoidosa*, and 70.79% RE was obtained by *S. abundans* (Brar et al. 2019b). It is possible that a significant amount of NH_4^+–N may be removed due to biological processes, such as bacterial nitrification, or physical

Table 4 Ammonium nitrogen removal efficiency obtained during the cultivation of *D. mucosa* VSPA and *C. pyrenoidosa* in different effluents

Wastewater source	*D. mucosa* VSPA			*C. pyrenoidosa*		
	Initial conc. (mg/L)	Final conc. (mg/L)	Removal efficiency (%)	Initial conc. (mg/L)	Final conc. (mg/L)	Removal efficiency (%)
TE1	45.2 ± 0.16	4.34 ± 0.07	90.4 ± 0.20	45.2 ± 0.16	7.34 ± 0.07	83.8 ± 0.20
TE2	54.6 ± 0.81	5.34 ± 0.07	90.2 ± 0.10	54.6 ± 0.81	8.67 ± 0.41	84.1 ± 1.00
TE3	46.2 ± 0.69	8.00 ± 0.53	82.7 ± 1.00	46.2 ± 0.69	10.34 ± 0.07	77.63 ± 0.30
Carpet effluents	83.8 ± 0.82	7.36 ± 0.86	94.0 ± 1.50	83.8 ± 0.82	11.69 ± 0.47	87.9 ± 0.70

Table 5 Phosphate–phosphorus removal efficiency obtained during the cultivation of *D. mucosa VSPA* and *C. pyrenoidosa* in different effluents

Wastewater source	*D. mucosa* VSPA			*C. pyrenoidosa*		
	Initial conc. (mg/L)	Final conc. (mg/L)	Removal efficiency (%)	Initial conc. (mg/L)	Final conc. (mg/L)	Removal efficiency (%)
TE1	5.47 ± 0.12	1.63 ± 0.05	70.1 ± 0.56	5.47 ± 0.12	1.92 ± 0.04	64.9 ± 0.50
TE2	6.43 ± 0.12	1.82 ± 0.09	71.6 ± 1.80	6.43 ± 0.12	2.14 ± 0.05	66.7 ± 1.00
TE3	7.8 ± 0.08	2.43 ± 0.12	68.8 ± 1.92	7.8 ± 0.12	2.9 ± 0.25	62.8 ± 3.30
Carpet effluents	9.37 ± 0.17	2.6 ± 0.08	71.6 ± 1.90	9.37 ± 0.17	3.13 ± 0.05	66.7 ± 1.00

processes, such as volatilization or sedimentation (Li et al. 2011; Delgadillo-Mirquez et al. 2016). But, in the control experiment, less than 10% of NH_4^+–N was removed, indicating that microalgae were solely responsible for removing a significant percent of NH_4^+–N.

Phosphate–phosphorus (PO_4^{3-}–P) removal efficiency (PRE)

Phosphorus present in wastewater is of two types: organic and inorganic. Inorganic phosphorus, or phosphate phosphorus (PO_4^{3-}–P), is transported into the cytosol by a specific transporter (Singh et al. 2019). In the cytosol, phosphate phosphorus can be converted into nucleic acid, protein, or insoluble granules, as shown in Figure S1. Hence, phosphorus is indirectly related to biomass production. Table 5 compares *D. mucosa* VSPA and *C. pyrenoidosa* for assimilating PO_4^{3-}–P from different wastewater sources. The pattern of removal is shown in Figure S3.

In this case, also, *D. mucosa* VSPA outperformed *C. pyrenoidosa* in all effluents, representing a better strain for the effluent treatment ($p < 0.05$). The efficiency of PO_4^{3-}–P removal by microalgae was less than that of NH_4^+–N because of the straightforward fact that the requirement of nitrogen by microalgae is greater; in contrast, only 1% (by weight) phosphate is present in algae biomass (Singh et al. 2023). It has also been reported that species belonging to the *Trebouxiophyceae* class can assimilate excess PO_4^{3-}–P present in the medium and store it in their vacuoles as polyphosphate granules. These granules can be used later in phosphorus-deficient conditions (Larsdotter 2006).

In carpet effluent, *D. mucosa* VSPA removed $71.6 \pm 1.9\%$ of PO_4^{3-}–P, while *C. pyrenoidosa* was able to remove $66.7 \pm 1.0\%$ of PO_4^{3-}–P. The final concentration of PO_4^{3-}–P reached 2.6 ± 0.08 mg/L in the case of *D. mucosa* VSPA and 3.13 ± 0.05 mg/L in the case of *C. pyrenoidosa* within 10 days of the cultivation period. Among the three variants of textile wastewater, similar to the case of ammonium nitrogen, the lowest PRE of $68.8 \pm 1.92\%$ and $62.8 \pm 3.3\%$ was obtained in the case of TE3 by *D. mucosa VSPA* and *C. pyrenoidosa*, respectively. At the same time, the highest PRE was obtained in TE2 by both species. They removed $71.6 \pm 1.8\%$ and $66.7 \pm 1.0\%$ phosphate, respectively. Brar et al. (2019) cultivated *C. pyrenoidosa* and *S. abundans* in 75% diluted textile wastewater for 25 days under batch conditions. *C. pyrenoidosa* was able to remove only 28.01% PO_4^{3-}–P, significantly less than the present case (Brar et al. 2019b). Similar to the case of NH_4^+–N, some portion of PO_4^{3-}–P may be eliminated due to some physical processes, such as chemical precipitation (Larsdotter et al. 2007). However, here also, less than 10% of PO_4^{3-}–P was eliminated in the control experiment, indicating that microalgae assimilated a significant portion of phosphate.

COD removal

Chemical oxygen demand (COD), a measurement of the organic load (strength of the effluent) in the wastewater and the amount of molten oxygen that may be used for its oxidation, is another key element in wastewater treatment (Otondo et al. 2018). In contrast to other common nutrients like nitrogen and phosphorus, the fate of COD during

Table 6 COD removal efficiency obtained during the cultivation of *D. mucosa VSPA* and *C. pyrenoidosa* in different effluents

Wastewater source	*D. mucosa* VSPA			*C. pyrenoidosa*		
	Initial conc. (mg/L)	Final conc. (mg/L)	Removal efficiency (%)	Initial conc. (mg/L)	Final conc. (mg/L)	Removal efficiency (%)
TE1	394 ± 4.30	81 ± 8.04	79.4 ± 2.20	394 ± 4.30	105 ± 2.50	73.3 ± 0.90
TE2	372 ± 3.20	70 ± 3.20	81.2 ± 0.70	372 ± 3.20	95 ± 2.50	74.4 ± 0.80
TE3	438 ± 8.16	104.6 ± 6.18	76.1 ± 1.60	438 ± 8.16	122.3 ± 7.85	72.1 ± 2.10
Carpet effluents	1568 ± 14.70	126.7 ± 5.25	91.9 ± 0.40	1568 ± 14.70	202.7 ± 13.10	87.1 ± 0.90

microalgal-based wastewater treatment has not been extensively characterised (Lee et al. 2019). The organic carbon is first transported to the cytosol by a specific transporter. Then, it is converted to L-glutamate and carbohydrate by the carbon centrate mechanism (Singh et al. 2019). Carbohydrate is used for energy production, and L-glutamate is used for biomass production, as shown in figure S1. Hence,

COD removal can be directly correlated with biomass production. Both species were compared for their COD removal efficiency in all effluents, and the obtained results are presented in Table 6. The pattern of COD removal is illustrated in Figure S4. A general trend can be observed: as the COD concentration increased, COD removal efficiency also increased. As the highest COD was detected in carpet effluent (1568 ± 14 mg/L), both species' highest COD removal efficiency was obtained in carpet effluent. *D. mucosa* VSPA

Table 7 Comparison of biomass production and pollutant removal efficiency by *D. mucosa* VSPA and *C. pyrenoidosa*

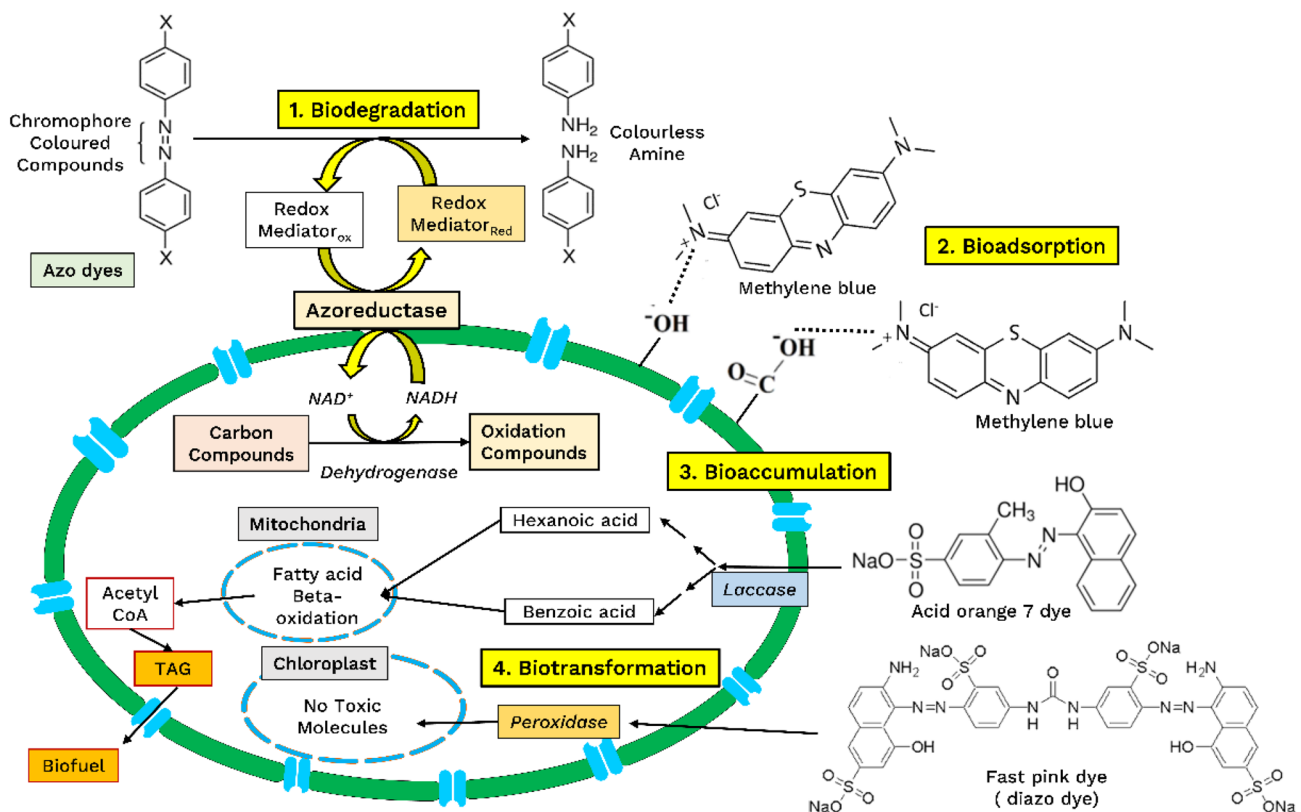| Wastewater source	Microalgae species							
	D. mucosa VSPA				*C. pyrenoidosa*			
	Removal efficiency (%)				Removal efficiency (%)			
	Biomass conc. (g/L)	NH_4^+–N	PO_4^{3-}–P	COD	Biomass conc. (g/L)	NH_4^+–N	PO_4^{3-}–P	COD
TE1	3.98	90.4	70.1	79.4	3.31	83.8	64.9	73.3
TE2	3.85	90.2	71.6	81.2	3.00	84.1	66.7	74.4
TE3	2.90	82.7	68.8	76.1	2.28	77.63	62.8	72.1
Carpet effluent	4.26	94.0	71.6	91.9	4.02	87.9	66.7	87.1

Fig. 3 Schematic diagram representing colour removal by microalgae via four mechanisms: (1) biodegradation (degradation into simpler compounds); (2) bio adsorption (adsorption on the cell surface); (3) bioaccumulation (conversion into simpler compounds and storage in cells for later use); (4) biotransformation (transformation into non-toxic compounds) (Fazal et al. 2018; Ishchi and Sibi 2019; Premaratne et al. 2021)
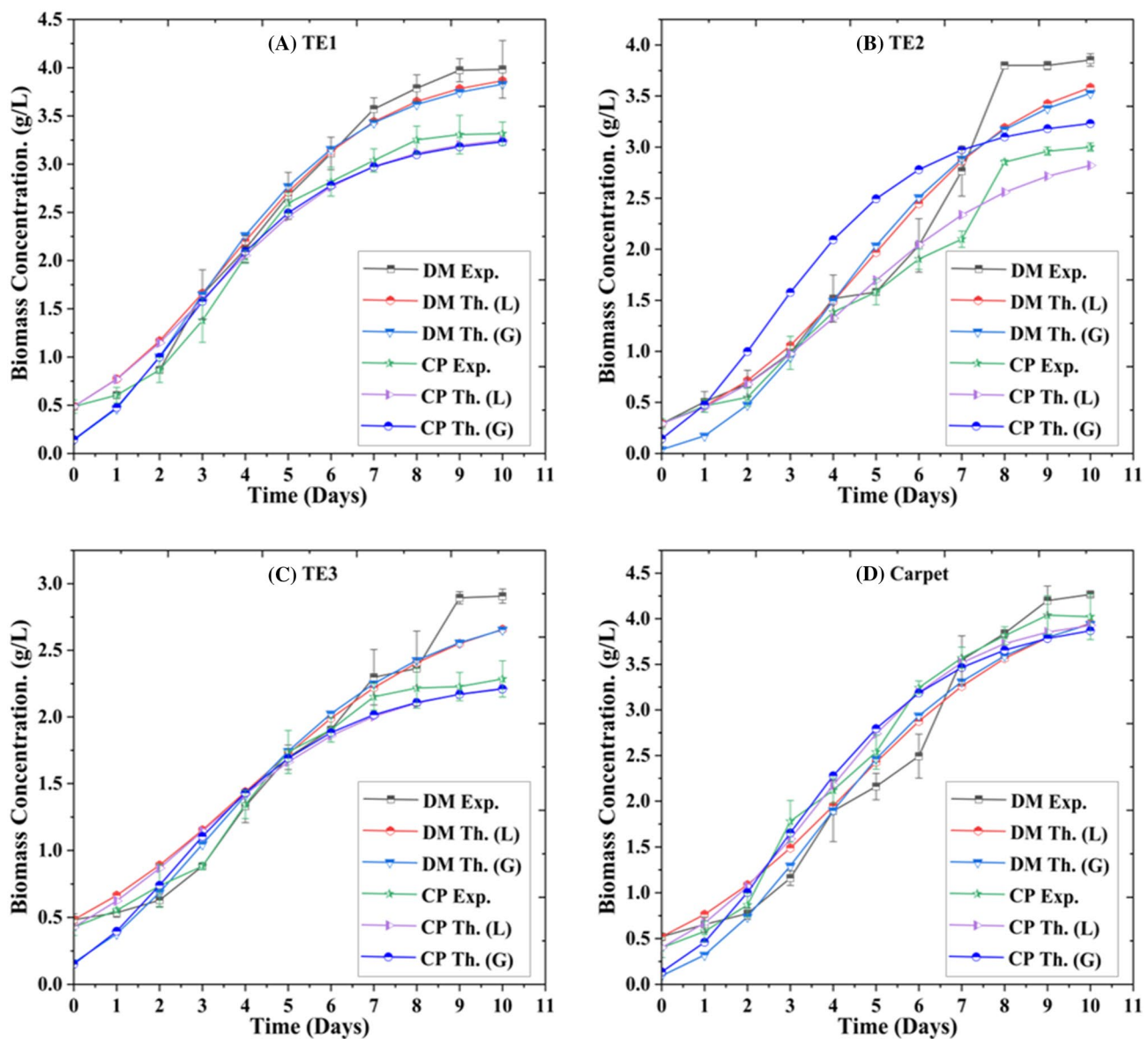
⁂ Springer

Fig. 4 Model simulation results obtained for biomass production: **A** textile effluent 1 (TE1); **B** textile effluent 2 (TE2); **C** textile effluent 3 (TE3); **D** carpet effluent; (DM: *D. mucosa* VSPA; CP: *Chlorella pyrenoidosa*; Exp.: experimental concentration; Th. (L) & Th. (G): theo-retical concentration obtained from photobiotreatment and Gompertz models). The photobiotreatment model was a better-fit model than Gompertz model

removed $91.9 \pm 0.4\%$ of COD, and $87.1 \pm 0.9\%$ of COD was removed by *C. pyrenoidosa*. The final concentration reached 126.70 ± 5.25 mg/L in *D. mucosa* VSPA culture, and 202.7 ± 13.1 mg/L in the case of *C. pyrenoidosa*. Notably, this is the first publication that reports COD removal from carpet effluent by microalgae.

In the case of textile effluent, similar to other pollutants, the highest COD RE was obtained in TE2. In comparison, the lowest was obtained in TE3. *D. mucosa VSPA* eradicated $81.2 \pm 0.7\%$ COD, while *C. pyrenoidosa* eradicated $74.4 \pm 0.8\%$ from the TE2. The results were analogous to

the previously reported findings. Wu et al. (2020) cultivated immobilised *Chlorella* sps. in different concentrations of textile wastewater in glass tubes. All species were able to remediate more than 75% of COD from the textile effluent (Wu et al. 2020). In another study, Behl et al. (2020) remediated effluent from a textile dyeing mill with an isolated *Chlamydomonas* sp. TRC-1. Complete colour removal was obtained within 7 days, with a COD removal efficiency of 83.08% (Behl et al. 2020). The release of organic molecules by microalgal cells will undoubtedly cause the COD of the sample to rise when the culture

Table 8 Colour removal efficiency obtained during the cultivation of *D. mucosa VSPA* and *C. pyrenoidosa* in different effluents

Wastewater source	*D. mucosa* VSPA			*C. pyrenoidosa*		
	Initial conc. (mg/L)	Final conc. (mg/L)	Removal efficiency (%)	Initial conc. (mg/L)	Final conc. (mg/L)	Removal efficiency (%)
TE1	140 ± 2.00	49 ± 1.00	65.5 ± 2.14	140 ± 2.30	56 ± 1.00	60.9 ± 1.30
TE2	180 ± 3.10	59 ± 1.00	67.0 ± 1.90	180 ± 0.20	66 ± 2.21	62.9 ± 0.96
TE3	200 ± 4.20	110 ± 2.00	54.7 ± 1.55	200 ± 3.10	102 ± 3	49.1 ± 0.71
Carpet effluents	95 ± 2.00	29 ± 1.00	69.2 ± 2.14	95 ± 1.10	34 ± 1.30	64.7 ± 2.01

enters the stationary phase. However, high removal efficiency in both cultures suggested that some COD may have been remedied by bacterial contamination, as shown in the control, or that newly forming microalgal cells may have assimilated the released organic content.

A summarised table comparing the efficiency of both species for the treatment of textile and carpet effluent is presented in Table 7.

Colour removal

The primary source of colour in wastewater is dyes, particularly in carpet and textile effluents (Fig. 3). Figure 4 represents the mechanism through which microalgae remediate dye from wastewater.

As depicted in Fig. 4, microalgal cells remediate colour from wastewater generally through four processes: (i) biodegradation; (ii) bioadsorption; (iii) bioaccumulation; and (iv) biotransformation. In biodegradation, dyes such as azo dyes are degraded by azoreductase enzyme into colourless and non-toxic amines (Ishchi and Sibi 2019). In the bioadsorption process, dyes are adsorbed on the cell surface due to opposite charge polarities on the cell surface and dyes (Fazal et al. 2018). Next, in the bioaccumulation process, dyes are converted into simpler carbon compounds via some enzyme, such as laccase (Fazal et al. 2018). Later, these compounds are metabolised by algal cells. Last, in the biotransformation process, the peroxidase enzyme transforms dye into non-toxic molecules (Premaratne et al. 2021). Table 8 represents the colour removal efficiency of various effluents.

As per the mechanism, it is clear that more growth will favour more colour removal. The highest colour removal was obtained in TE2 by both species, which was $67.00 \pm 1.90\%$ in *D. mucosa* VSPA culture, while $62.90 \pm 0.96\%$ removal was obtained in *C. pyrenoidosa* culture. The lowest was obtained in the TE3, which was $54.70 \pm 1.55\%$ in *D. mucosa* VSPA, while removal efficiency reached $49.10 \pm 0.71\%$ in *C. pyrenoidosa* culture. In the remaining effluents (carpet, domestic, and petroleum), more than 70% colour removal efficiency was obtained in the *D. mucosa* VSPA culture. In comparison, more than 65% colour remediation was obtained in *C. pyrenoidosa* cultures.

Modelling study

Two models, the PhBT and Gompertz models, were used for modelling the study and validating the experimental results. In addition to R^2 values, AICC values are used to compare theoretical models better. Table S2 and Fig. 4 represent the modelling simulation study for biomass production.

R^2 and RMSE (root mean square error) values indicated that both models better fitted the experimental results. But, AICC values indicate that the PhBT model provides a better fit than the Gompertz model. Maximum specific growth (*p*), as revealed by the PhBT model, was highest in carpet effluent for both species and lowest in TE3. It was even higher for the *D. mucosa* VSPA strain. The results of kinetic parameters were reflected in biomass concentration results, as the highest biomass concentration was obtained in carpet effluent. *p* is one of the critical parameters for deciding the dilution rate and flow rate during the design of a continuous reactor. Also, as revealed by the Gompertz model, the lag phase duration was low in carpet effluent compared to textile effluent.

Model simulation studies for nutrient removal is represented in Tables S3 and S4 and Figs. 5 and 6, respectively.

Here, too, the AICC value indicated that the PhBT model better fits the experimental data of pollutant removal compared to the Gompertz model. p values obtained during the model simulation study also indicate that the *D. mucosa* strain has a high growth rate. Even if the investigated nutrient is not limiting, the PhBT model can still be used for nitrogen and phosphorus. Although it hasn't been empirically proven in this study, theoretically, the model might be used for any nutrient readily available in a finite concentration. The PhBT model can calculate the maximum number of nutrient reserves throughout the experiment and the microalgae's
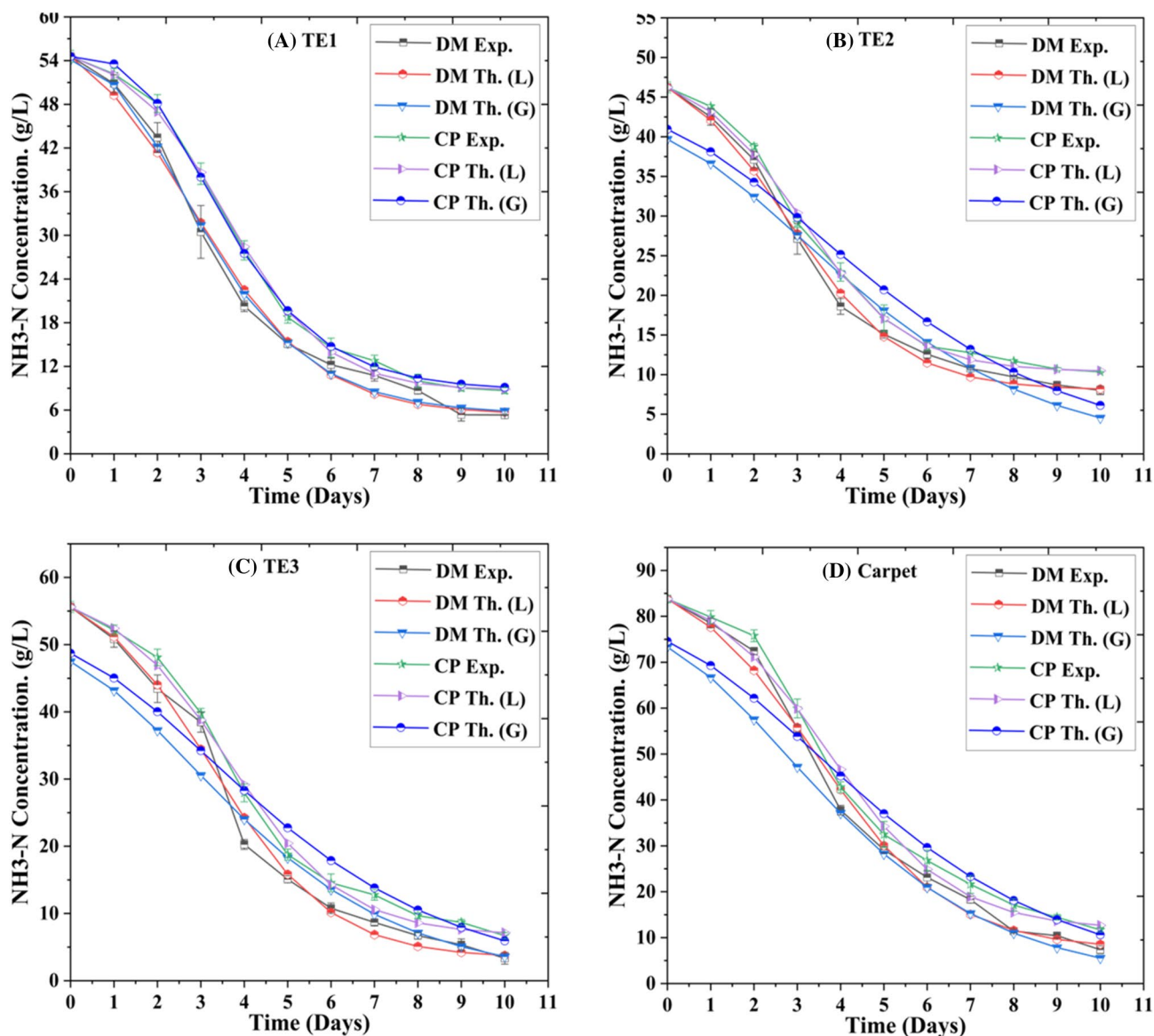
Fig. 5 Model simulation results obtained for ammonium nitrogen removal: **A** textile effluent 1 (TE1); **B** textile effluent 2 (TE2); **C** textile effluent 3 (TE3); **D** carpet effluent; (DM: *D. mucosa* VSPA; CP: *Chlorella pyrenoidosa*; Exp.: experimental concentration; Th. (L) & Th. (G): theoretical concentration obtained from photobiotreatment and Gompertz models. Here also, the photobiotreatment model was a better-fit model than Gompertz model

luxurious uptake of nutrients. Consideration should be given to implementing a suitable cultivation mode during wastewater treatment, where the primary goal is the removal of nutrients rather than maximising biomass production (Ruiz et al. 2013). In some cases, the Gompertz model also provided a better fit to the experimental data. This might indicate a chance of nutrient removal through physical processes such as adsorption by microalgae biomass.

Conclusion

In the present study, two microalgal strains, *D. mucosa VSPA* and *C. pyrenoidosa, were* compared for their growth and treatment efficiency of textile and carpet effluent cultivated in conventionally designed bubble column PBR. *D. mucosa VSPA* proved to be a superior strain than *C. pyrenoidosa*, with the final biomass concentration reaching 4.26 g/L in carpet effluent. Current treatment technology provides better removal efficiency of pollutants, including more than 85%
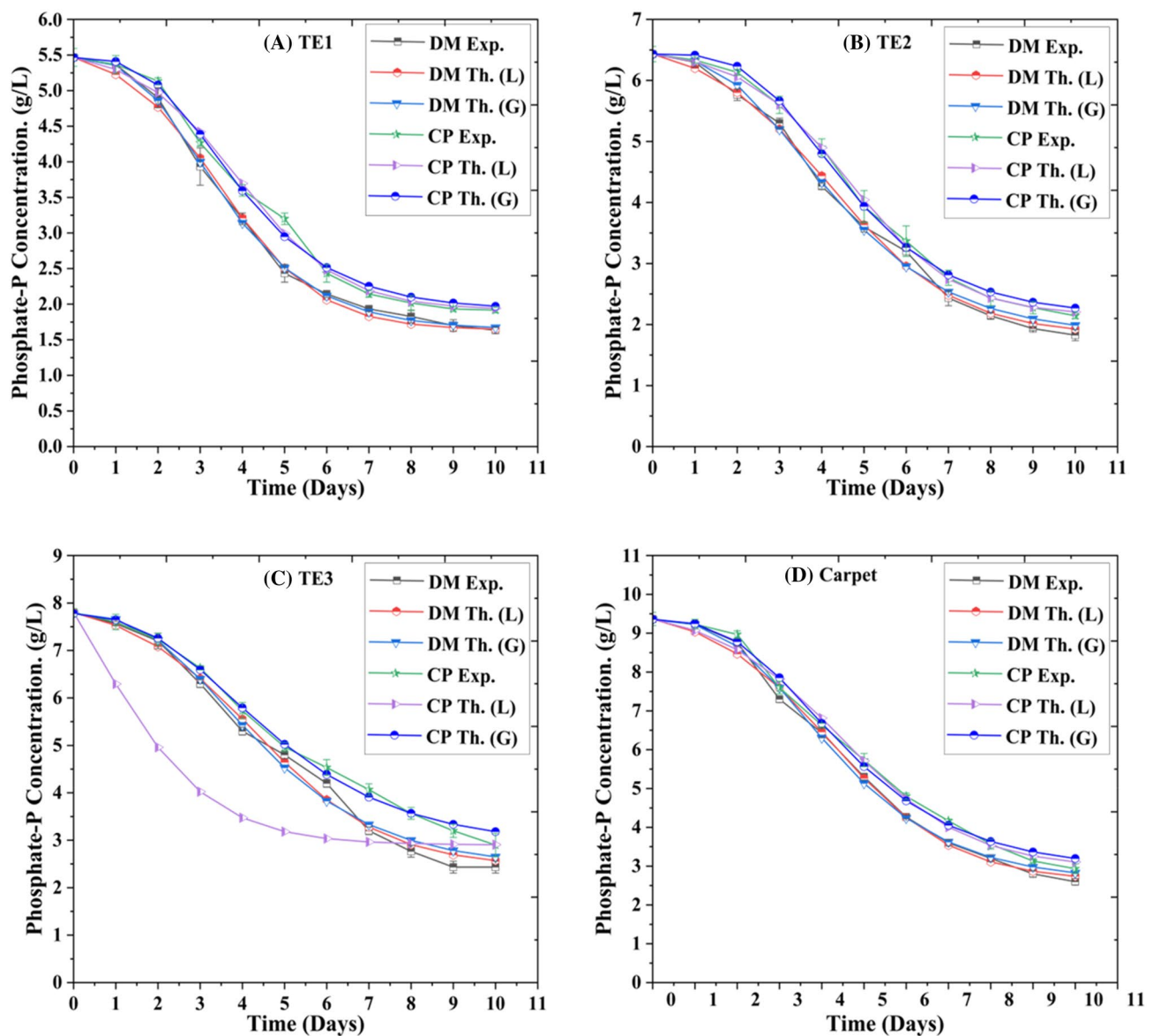
Fig. 6 Model simulation results obtained for phosphate phosphorus removal: **A** textile effluent 1 (TE1); **B** textile effluent 2 (TE2); **C** textile effluent 3 (TE3); **D** carpet effluent; (DM: *D. mucosa* VSPA; CP: *Chlorella pyrenoidosa*; Exp.: experimental concentration; Th. (P) & Th. (G): theoretical concentration obtained from photobiotreatment and Gompertz models. Here also, the photobiotreatment model was a better-fit model than Gompertz model

removal of ammonium nitrogen, 70% of phosphate phosphorus, 75% of COD, and 60% of colour from all effluent. The PhBT model better fits the experimental data, providing some critical design parameters. The study can be expanded by testing more unexplored microalgae strains to treat various industrial effluents. Dumping points in industries can be a potential source of unexplored strains. Also, the discussed design parameters of the bubble column reactor will assist future studies in the easy scale-up of the photobioreactors.

Data availability statement The data used in the research is confidential.

Declarations

Conflict of interest The authors declare that they have no known competing financial interests or personal relationships that could have appeared to influence the work reported in this paper. I hereby declare that there is no potential conflict of interest among all authors.

Ethical statements The manuscript should not be submitted to more than one publication for simultaneous consideration.

References

Baquerisse D, Nouals S, Isambert A, et al (1999) Modelling of a continuous pilot photobioreactor for microalgae production. In: Osinga R, Tramper J, Burgess JG, Wijffels RHBT-P in IM (eds) Marine bioprocess engineering. Elsevier, pp 335–342. https://doi.org/10.1016/S0079-6352(99)80125-8

Behera B, Acharya A, Gargey IA et al (2019) Bioprocess engineering principles of microalgal cultivation for sustainable biofuel production. Bioresour Technol Rep 5:297–316. https://doi.org/10.1016/j.biteb.2018.08.001

Behl K, SeshaCharan P, Joshi M et al (2020) Multifaceted applications of isolated microalgae *Chlamydomonas* sp. TRC-1 in wastewater remediation, lipid production and bioelectricity generation. Bioresour Technol 304:122993. https://doi.org/10.1016/j.biortech.2020.122993

Bischoff HW (1963) Phycological studies. IV. Some algae from enchanted rock and related algal species. Univ Texas Publ 6318:95

Brar A, Kumar M, Pareek N (2019a) Comparative appraisal of biomass production, remediation, and bioenergy generation potential of microalgae in dairy wastewater. Front Microbiol 10:678. https://doi.org/10.3389/fmicb.2019.00678

Brar A, Kumar M, Vivekanand V, Pareek N (2019b) Phycoremediation of textile effluent-contaminated water bodies employing microalgae: nutrient sequestration and biomass production studies. Int J Environ Sci Technol 16:7757–7768. https://doi.org/10.1007/s13762-018-2133-9

Chinnasamy S, Bhatnagar A, Hunt RW, Das KC (2010) Microalgae cultivation in a wastewater dominated by carpet mill effluents for biofuel applications. Bioresour Technol 101:3097–3105. https://doi.org/10.1016/j.biortech.2009.12.026

Delgadillo-mirquez L, Lopes F, Taidi B, Pareau D (2016) Nitrogen and phosphate removal from wastewater with a mixed microalgae and bacteria culture. Biotechnol Rep 11:18–26. https://doi.org/10.1016/j.btre.2016.04.003

El-Kassas HY, Mohamed LA (2014) Bioremediation of the textile waste effluent by *Chlorella vulgaris*. Egypt J Aquat Res 40:301–308. https://doi.org/10.1016/j.ejar.2014.08.003

Fazal T, Mushtaq A, Rehman F et al (2018) Bioremediation of textile wastewater and successive biodiesel production using microalgae. Renew Sustain Energy Rev 82:3107–3126. https://doi.org/10.1016/j.rser.2017.10.029

Fu W, Gudmundsson O, Feist AM et al (2012) Maximizing biomass productivity and cell density of *Chlorella vulgaris* by using light-emitting diode-based photobioreactor. J Biotechnol 161:242–249. https://doi.org/10.1016/j.jbiotec.2012.07.004

Han P, Lu Q, Zhong H et al (2021) Recycling nutrients from soy sauce wastewater to culture value-added *Spirulina maxima*. Algal Res 53:102157. https://doi.org/10.1016/j.algal.2020.102157

Hemalatha M, Sravan JS, Min B, Venkata Mohan S (2019) Microalgae-biorefinery with cascading resource recovery design associated to dairy wastewater treatment. Bioresour Technol 284:424–429. https://doi.org/10.1016/j.biortech.2019.03.106

Huang Q, Jiang F, Wang L, Yang C (2017) Design of photobioreactors for mass cultivation of photosynthetic organisms. Engineering 3:318–329. https://doi.org/10.1016/J.ENG.2017.03.020

Ishchi T, Sibi G (2019) Azo dye degradation by *Chlorella vulgaris*: optimization and kinetics. J Biol Chem 14:1–7. https://doi.org/10.3923/ijbc.2020.1.7

Japar AS, Takriff MS, Mohd Yasin NH (2021) Microalgae acclimatization in industrial wastewater and its effect on growth and primary metabolite composition. Algal Res 53:102163. https://doi.org/10.1016/J.ALGAL.2020.102163

Jones SMJ, Harrison STL (2014) Aeration energy requirements for lipid production by *Scenedesmus* sp. in airlift bioreactors. Algal Res 5:249–257. https://doi.org/10.1016/j.algal.2014.03.003

Jose S, Archanaa S (2019) Phycoremediation of textile wastewater: possibilities and constraints BT—application of microalgae in wastewater treatment: volume 1: domestic and industrial wastewater treatment. In: Gupta SK, Bux F (eds) Springer International Publishing, Cham, pp 291–319. https://doi.org/10.1007/978-3-030-13913-1_14

Khoo CG, Lam MK, Lee KT (2016) Pilot-scale semi-continuous cultivation of microalgae *Chlorella vulgaris* in bubble column photobioreactor (BC-PBR): hydrodynamics and gas-liquid mass transfer study. Algal Res 15:65–76. https://doi.org/10.1016/j.algal.2016.02.001

Klausmeier CA, Litchman E, Daufresne T, Levin SA (2004) Optimal nitrogen-to-phosphorus stoichiometry of phytoplankton. Nature 429:171–174. https://doi.org/10.1038/nature02454

Krishnamoorthy S, Manickam P, Muthukaruppan V (2019) Evaluation of distillery wastewater treatability in a customized photobioreactor using blue-green microalgae—laboratory and outdoor study. J Environ Manag 234:412–423. https://doi.org/10.1016/j.jenvman.2019.01.014

Larsdotter K (2006) Wastewater treatment with microalgae—a literature review. Vatten 62:31–38

Larsdotter K, la Cour JJ, Dalhammar G (2007) Biologically mediated phosphorus precipitation in wastewater treatment with microalgae. Environ Technol 28:953–960. https://doi.org/10.1080/09593332808618855

Lee SA, Lee N, Oh HM, Ahn CY (2019) Enhanced and balanced microalgal wastewater treatment (COD, N, and P) by interval inoculation of activated sludge. J Microbiol Biotechnol 29:1434–1443. https://doi.org/10.4014/JMB.1905.05034

Leng L, Wei L, Xiong Q et al (2020) Use of microalgae-based technology for the removal of antibiotics from wastewater: a review. Chemosphere 238:124680. https://doi.org/10.1016/j.chemosphere.2019.124680

Li Y, Chen Y-FF, Chen P et al (2011) Characterization of a microalga *Chlorella* sp. well adapted to highly concentrated municipal wastewater for nutrient removal and biodiesel production. Bioresour Technol 102:5138–5144. https://doi.org/10.1016/j.biortech.2011.01.091

López-Rosales L, García-Camacho F, Sánchez-Mirón A et al (2017) Modeling shear-sensitive dinoflagellate microalgae growth in bubble column photobioreactors. Bioresour Technol 245:250–257. https://doi.org/10.1016/j.biortech.2017.08.161

Martínez Sancho MAE, Jiménez Castillo JM, el Yousfi F (1997) Influence of phosphorus concentration on the growth kinetics and stoichiometry of the microalga *Scenedesmus obliquus*.

Process Biochem 32:657–664. https://doi.org/10.1016/S0032-9592(97)00017-4

Mayers JJ, Flynn KJ, Shields RJ (2014) Influence of the N:P supply ratio on biomass productivity and time-resolved changes in elemental and bulk biochemical composition of *Nannochloropsis* sp. Bioresour Technol 169:588–595. https://doi.org/10.1016/j.biortech.2014.07.048

Mazhar S, Ditta A, Bulgariu L et al (2019) Sequential treatment of paper and pulp industrial wastewater: prediction of water quality parameters by Mamdani fuzzy logic model and phytotoxicity assessment. Chemosphere 227:256–268. https://doi.org/10.1016/J.CHEMOSPHERE.2019.04.022

Mehmood MA, Rashid U, Ibrahim M, et al (2014) Algal biomass production using waste water BT—biomass and bioenergy: processing and properties. In: Hakeem KR, Jawaid M, Rashid U (eds) Springer International Publishing, Cham, pp 307–327

Mohammadi M, Mowla D, Esmaeilzadeh F, Ghasemi Y (2019) Enhancement of sulfate removal from the power plant wastewater using cultivation of indigenous microalgae: Stage-wise operation. J Environ Chem Eng 7:102870. https://doi.org/10.1016/j.jece.2018.102870

Mohsenpour SF, Hennige S, Willoughby N et al (2021) Integrating micro-algae into wastewater treatment: A review. Sci Total Environ 752:142168. https://doi.org/10.1016/j.scitotenv.2020.142168

Organization WH (2022) Guidelines for drinking-water quality: incorporating the first and second addenda. World Health Organization, Geneva

Otondo A, Kokabian B, Stuart-Dahl S, Gude VG (2018) Energetic evaluation of wastewater treatment using microalgae, *Chlorella vulgaris*. J Environ Chem Eng 6:3213–3222. https://doi.org/10.1016/j.jece.2018.04.064

Pathak VV, Kothari R, Chopra AK, Singh DP (2015) Experimental and kinetic studies for phycoremediation and dye removal by *Chlorella pyrenoidosa* from textile wastewater. J Environ Manag 163:270–277. https://doi.org/10.1016/j.jenvman.2015.08.041

Patil SS, Behera B, Sen S, Balasubramanian P (2021) Performance evaluation of bubble column photobioreactor along with CFD simulations for microalgal cultivation using human urine. J Environ Chem Eng 9:104615. https://doi.org/10.1016/j.jece.2020.104615

Pena ACC, Agustini CB, Trierweiler LF, Gutterres M (2020) Influence of period light on cultivation of microalgae consortium for the treatment of tannery wastewaters from leather finishing stage. J Clean Prod 263:121618. https://doi.org/10.1016/j.jclepro.2020.121618

Premaratne M, Nishshanka GKSH, Liyanaarachchi VC et al (2021) Bioremediation of textile dye wastewater using microalgae: current trends and future perspectives. J Chem Technol Biotechnol 96:3249–3258. https://doi.org/10.1002/jctb.6845

Raabová L, Elster J, Kováčik L (2016) Phototrophic microflora colonizing substrates of man-made origin in Billefjorden Region, Central Svalbard. Czech Polar Rep 6:21–30. https://doi.org/10.5817/CPR2016-1-3

Rice EW, Bridgewater L, Association APH (2012) Standard methods for the examination of water and wastewater. American Public Health Association, Washington, DC

Ruiz J, Arbib Z, Álvarez-Díaz PD et al (2013) Photobiotreatment model (PhBT): a kinetic model for microalgae biomass growth and nutrient removal in wastewater. Environ Technol 34:979–991. https://doi.org/10.1080/09593330.2012.724451

Sánchez Mirón A, García Camacho F, Contreras Gómez A et al (2000) Bubble-column and airlift photobioreactors for algal culture. AIChE J 46:1872–1887. https://doi.org/10.1002/aic.690460915

Santiago AF, Calijuri ML, Assemany PP et al (2013) Algal biomass production and wastewater treatment in high-rate algal ponds receiving disinfected effluent. Environ Technol 34:1877–1885. https://doi.org/10.1080/09593330.2013.812670

Sanz-Luque E, Chamizo-Ampudia A, Llamas A et al (2015) Understanding nitrate assimilation and its regulation in microalgae. Front Plant Sci 6:899. https://doi.org/10.3389/fpls.2015.00899

Schmidt JJ (2019) Valuing water: rights, resilience, and the UN high-level panel on water. Water politics. Routledge, London, pp 15–27

Singh V, Mishra V (2019) Bioremediation of nutrients and heavy metals from wastewater by microalgal cells: mechanism and kinetics BT—microbial genomics in sustainable agroecosystems: volume 2. In: Tripathi V, Kumar P, Tripathi P et al (eds) Springer Singapore, Singapore, pp 319–357

Singh V, Mishra V (2020) Enhanced biomass production and nutrient removal efficiency from urban wastewater by *Chlorella pyrenoidosa* in batch bioreactor system: optimization and model simulation. Desalination Water Treat 2:1–39. https://doi.org/10.5004/dwt.2020.25967

Singh V, Mishra A, Srivastava P (2023) Textile and domestic effluent treatment via co-cultivation of *Diplosphaera mucosa* VSPA and *Scenedesmus obliquus*. Biomass Bioenergy 172:106756. https://doi.org/10.1016/j.biombioe.2023.106756

Song C, Hu X, Liu Z et al (2020) Combination of brewery wastewater purification and CO_2 fixation with potential value-added ingredients production via different microalgae strains cultivation. J Clean Prod 268:122332. https://doi.org/10.1016/j.jclepro.2020.122332

Sturm BSM, Lamer SL (2011) An energy evaluation of coupling nutrient removal from wastewater with algal biomass production. Appl Energy 88:3499–3506. https://doi.org/10.1016/j.apenergy.2010.12.056

Tuantet K, Temmink H, Zeeman G et al (2019) Optimization of algae production on urine. Algal Res 44:101667. https://doi.org/10.1016/j.algal.2019.101667

Venkatesan J, Manivasagan P, Kim S-K (2015) Marine microalgae biotechnology: present trends and future advances. Handbook of marine microalgae. Elsevier, Amsterdam, pp 1–9

Vidyarthi AK, Kumar P, Negi S, Kumar V (2020) Wastewater characterization of grossly polluted textile industries located at main stem of river Ganga in Uttar Pradesh, India. Ecol Environ Conserv 26:S378–S381

Wágner DS, Cazzaniga C, Steidl M et al (2021) Optimal influent N-to-P ratio for stable microalgal cultivation in water treatment and nutrient recovery. Chemosphere 262:127939. https://doi.org/10.1016/j.chemosphere.2020.127939

Wan J, Gu J, Zhao Q, Liu Y (2016) COD capture: a feasible option towards energy self-sufficient domestic wastewater treatment. Sci Rep 6:25054. https://doi.org/10.1038/srep25054

Wu JY, Lay CH, Chiong MC et al (2020) Immobilized *Chlorella* species mixotrophic cultivation at various textile wastewater concentrations. J Water Process Eng 38:101609. https://doi.org/10.1016/j.jwpe.2020.101609

Xu L, Weathers PJ, Xiong X-R, Liu C-Z (2009) Microalgal bioreactors: challenges and opportunities. Eng Life Sci 9:178–189. https://doi.org/10.1002/elsc.200800111

Yadav G, Dash SK, Sen R (2019) A biorefinery for valorization of industrial wastewater and flue gas by microalgae for waste mitigation, carbon-dioxide sequestration and algal biomass production.

Sci Total Environ 688:129–135. https://doi.org/10.1016/j.scitotenv.2019.06.024

You X, Yang L, Zhou X, Zhang Y (2022) Sustainability and carbon neutrality trends for microalgae-based wastewater treatment: a review. Environ Res 209:112860. https://doi.org/10.1016/j.envres.2022.112860